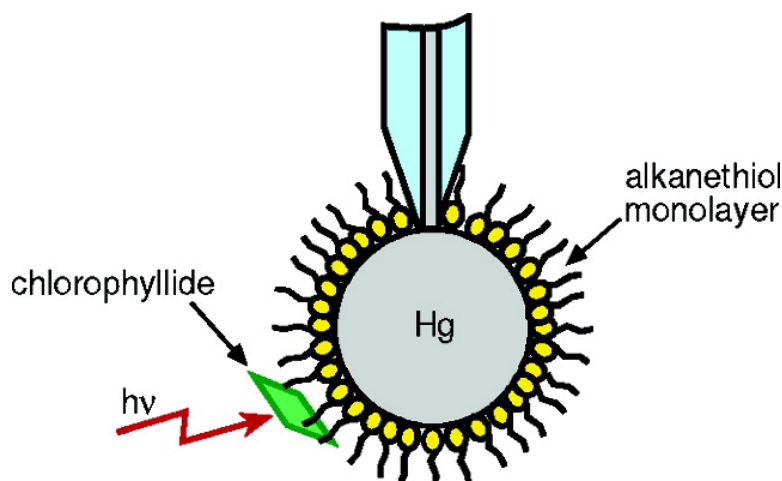Article

Photoinduced Electroreduction of Chlorophyllide on Alkanethiol-Coated Mercury

Francesco Tadini Buoninsegni, Maria Rosa Moncelli, Giovanni Aloisi, Angela Agostiano, and Rolando Guidelli

More About This Article

Additional resources and features associated with this article are available within the HTML version:

- Supporting Information
- Access to high resolution figures
- Links to articles and content related to this article
- Copyright permission to reproduce figures and/or text from this article

View the Full Text HTML

Photoinduced Electroreduction of Chlorophyllide on Alkanethiol-Coated Mercury

Francesco Tadini Buoninsegni,[†] Maria Rosa Moncelli,[†] Giovanni Aloisi,[†]
Angela Agostiano,[‡] and Rolando Guidelli*,[†]

*Contribution from the Departments of Chemistry, University of Florence, Via della Lastruccia 3,
50019 Sesto Fiorentino, Florence, Italy, and University of Bari,
Via Orabona 4, 70125 Bari, Italy*

Received July 26, 2004; E-mail: guidelli@unifi.it

Abstract: Monolayers of *n*-alkanethiols of chain length from C_{12} to C_{18} were self-assembled on a hanging mercury drop electrode, and a film of chlorophyllide (Chlide) was adsorbed on top of them. The reduction photocurrents following illumination of the Chlide film were measured over the potential range in which the Chlide is electroinactive in the dark, and their action spectra were determined. Plotting the derivative of the photocurrents with respect to the applied potential against potential yields bell-shaped curves that can be fitted to a Gaussian. The potential of the Gaussian maximum was used to determine the reorganization energy λ for the Chlide electroreduction process. An increase in the thiol chain length causes λ to decrease regularly and the photocurrent to decay exponentially with the monolayer thickness, with a decay constant β of about 0.17 Å^{-1}.

Introduction

Chlorophyll (Chl) is a pigment present in the thylacoid membrane of higher plants that plays a fundamental role in photosynthesis. In the excited state Chl is both a strong reductant and a strong oxidant.

A Chl film self-assembled directly on mercury from its solution in hexane, once illuminated with red light in a pH 8.5 aqueous solution of 0.1 M KCl, yields a photocurrent that depends notably upon the applied potential.[1] Thus, at −0.160 V/SCE, the light-on current is negative, namely it corresponds to a flow of negative charges from the electrode toward the solution. Proceeding toward more negative applied potentials, the light-on current first increases, attaining a maximum value at about −0.460 V/SCE, but then decreases with a further negative shift in the applied potential until, ultimately, it starts passing from negative to positive values. This photoelectro-chemical behavior, combined with chronocoulometric measurements of Chl electroreduction in the dark, was interpreted by assuming that, at less negative potentials, a film of adsorbed Chl dimers mediates electron transfer from the electrode to water, with hydrogen evolution.[1] In the proximity of −0.800 V/SCE, an incipient Chl electroreduction causes cleavage of the H-bond between the Chl units of the dimers and reorientation of the resulting units. Such a reorientation seems to favor electron transfer from the photoexcited Chl molecules to the metal, rather than to water. The resulting Chl$^+$ cations may then oxidize water with oxygen evolution.

In the reaction center of photosynthetic bacteria, an electron is transferred from the excited bacteriochlorophylls of the special pair to a bacteriopheophytin, likely involving participation of an ancillary BChl whose exact role is still controversial. On the other side, the Chl$^+$ cation may accept an electron from semiquinone radicals across distances that may range from 4.5 to 23 Å.[2] Such a variation of about 20 Å in the distance between donors and acceptors in the protein changes the electron-transfer rate by about 10^{12}-fold. It is now generally accepted that electron transfer across relatively large distances takes place via through-bond tunneling, where both covalent and hydrogen bonds may be involved.[3−6] In view of the structural complexity of proteins, model systems have been employed in which the distance between donor and acceptor and the nature of the intermediate medium are varied under controlled conditions. Thus, fatty acid monolayers have been employed as spacers between donors and acceptors in photoreduction experiments.[7−10] Countless experiments aiming at investigating electron tunneling have been carried out by using a gold electrode as an electron donor or acceptor (for an exhaustive review, see ref 11); this was separated from a redox couple by a self-assembled monolayer

---

[†] University of Florence.
[‡] University of Bari.

(1) Tadini Buoninsegni, F.; Becucci, L.; Moncelli, M. R.; Guidelli, R.; Agostiano, A.; Cosma, P. *J. Electroanal. Chem.* **2003**, *550−551*, 229−240.

(2) Moser, C. C.; Keske, J. M.; Warncke, K.; Farid, R. S.; Leslie Dutton, P. *Nature* **1992**, *355*, 796−802.
(3) Beratan, D. N.; Betts, J. N.; Onuchic, J. N. *Science* **1991**, *252*, 1285−1288.
(4) Onuchic, J. N.; Beratan, D. N.; Winkler, J. R.; Gray, H. B. *Annu. Rev. Biophys. Biomol. Struct.* **1992**, *21*, 349−377.
(5) Beratan, D. N.; Onuchic, J. N.; Winkler, J. R.; Gray, H. B. *Science* **1992**, *258*, 1740−1741.
(6) Langen, R.; Chang, I.-J.; Germanas, J. P.; Richards, J. H.; Winkler, J. R.; Gray, H. B. *Science* **1995**, *268*, 1733−1735.
(7) Sugi, M.; Nembach, K.; Möbius, D.; Khun, H. *Solid State Commun.* **1974**, *15*, 1867−1870.
(8) Khun, H. *J. Photochem.* **1979**, *10*, 111−132.
(9) Killesreiter, H.; Baessler, H. *Chem. Phys. Lett.* **1971**, *11*, 411−414.
(10) Khanova, L. A.; Tarasevich, M. R. *J. Electroanal. Chem.* **1987**, *227*, 115−127.

(SAM) of alkanethiol derivatives of different chain lengths, so as to vary the donor−acceptor distance in a controlled way. These electrochemical systems, which have been employed almost exclusively with photoinactive redox couples, have the advantage of allowing the standard free energy of the reaction to be varied continuously by merely varying the applied potential.

Mercury has a homogeneous, featureless, defect-free surface that lends itself to the formation of well-behaved SAMs, which are extremely blocking toward both hydrophilic and hydrophobic redox couples and are almost free from pinholes.[12−14] This is an indisputable advantage of Hg over solid electrodes such as gold, whose surface steps and kinks are responsible for defects in the deposited films. Moreover, mercury electrodes are readily renewable and do not require conditioning prior to use. In a preliminary investigation carried out in the present laboratory,[15] photocurrents obtained by illuminating a Chl film deposited on top of mercury-supported SAMs of alkanethiols of chain length from C_{12} to C_{18} were measured to verify the effect of the potential energy barrier created by these monolayers of different thicknesses upon the transfer of the Chl photoexited electron. Due to the insolubility of Chl in aqueous solutions, Chl was adsorbed on the thiol SAMs from a 50% (v/v) ethanol−water mixture, and the thiol-coated mercury drop was then transferred to an aqueous solution. The amount of Chl adsorbed on the thiol SAMs was found to be not entirely reproducible. Satisfactory results were obtained with dodecanethiol and tetradecanethiol SAMs, whose liquid-like nature allows the phytyl chains of Chl to intercalate within the alkanethiol chains.

This work reports an analogous investigation carried out with chlorophyllide (Chlide), a Chl molecule lacking the phytyl side chain. This molecule is slightly soluble in water, so as to be adsorbed on top of the SAM-coated mercury directly from the working aqueous solution, with a resulting increase in reproducibility. Action spectra of the stationary photocurrent of Chlide were measured. Photocurrents of Chlide adsorbed on dodecanethiol and tetradecanethiol SAMs were recorded while gradually expanding the supporting mercury drop, so as to increase the tilt of the alkanethiol molecules.

Experimental Section

Chemicals. The water used was obtained from water produced by an inverted osmosis unit by distilling it once and then distilling the resulting water from alkaline permanganate, while discarding the heads. Merck reagent grade KCl was baked at 500 °C before use to remove any organic impurities. All inorganic salts were purchased from Merck; *n*-alkanethiols from Fluka were used without further purification. The pH 8.5 aqueous solutions used in Chlide photocurrent measurements were buffered with 5×10^{-3} M H_3BO_3 + 1.2×10^{-3} M NaOH.

Experimental Setup and Procedures. The experimental setup employed in photocurrent measurements of Chlide is described in refs 1 and 15, and the thermostated homemade hanging mercury drop electrode (HMDE) is described in ref 16. In the present measurements, the mercury drop had a surface area of 1.4×10^{-2} cm².

(11) Finklea, H. O. In *Electroanalytical Chemistry*; Bard, A. J., Rubinstein, I., Eds.; Marcel Dekker: New York, 1996; Vol. 19, pp 109−335.
(12) Demoz, A.; Harrison, D. J. *Langmuir* **1993**, *9*, 1046−1050.
(13) Tadini Buoninsegni, F.; Herrero, R.; Moncelli, M. R. *J. Electroanal. Chem.* **1998**, *452*, 33−42.
(14) Tadini Buoninsegni, F.; Becucci, L.; Moncelli, M. R.; Guidelli, R. *J. Electroanal. Chem.* **2001**, *500*, 395−407.
(15) Tadini Buoninsegni, F.; Dolfi, A.; Guidelli, R. *Collect. Czech. Chem. Commun.* **2004**, *69*, 292−308.
(16) Moncelli, M. R.; Becucci, L. *J. Electroanal. Chem.* **1997**, *433*, 91−96.

Table 1. Differential Capacity and Resistance of Alkanethiol SAMs of Different Chain Lengths, Potential of the Gaussian Maximum, and Reorganization Energy, λ, for Chlide-Photoinduced Electroreduction on These SAMs

	C_{12}SH	C_{14}SH	C_{16}SH	C_{18}SH
C (μF cm^{-2})	1.04	0.88	0.79	0.70
R (MΩ cm²)	0.20	0.50	2.45	2.65
E (V vs Ag|AgCl|0.1M KCl)	−0.76	−0.62	−0.50	−0.41
λ (eV)	0.96	0.82	0.70	0.61

Alkanethiol monolayers on mercury were prepared by the "soaking procedure". According to this procedure, the alkanethiol coating was obtained by immersing the mercury drop in a 20% (v/v) solution of the alkanethiol in ethanol or chloroform for 1 min; the thiol-coated mercury drop was then usually rinsed with chloroform or ethanol to remove unadsorbed alkanethiol and immersed into the electrolytic solution. Alkanethiols with 12, 14, 16, and 18 carbon atoms (henceforth briefly denoted by C_{12}, C_{14}, C_{16}, and C_{18}) were employed. The capacitance C and resistance R of each thiol monolayer were estimated by impedance spectroscopy measurements with a Stanford Research SR850 lock-in amplifier, upon representing the alkanethiol monolayer as an RC mesh. The R and C values of the alkanethiol monolayers are summarized in Table 1. The thiol-coated HMDE was then immersed in a small Plexiglas cell containing an aqueous solution of 4.72×10^{-6} M Chlide and 0.1 M KCl, buffered at pH 8.5. The Chlide was allowed to adsorb on the thiol-coated mercury for 30 min and was then photoexcited with red light. To this end, the Plexiglas cell was provided with a quartz optical fiber (0.6 mm in diameter), whose tip was positioned on the cell bottom and was pointed vertically toward the HMDE for its illumination. For a good alignment of the optical fiber with the mercury drop, the cell was mounted on an x−y slide. The monochromatic light source (red light laser, 670 nm, Electron model LA5-3.5G-670) was focused and collimated using an optical fiber coupler (Newport model F-915T). Light pulses were produced using an electromechanical shutter (blade shutter and digital shutter controller, Newport model 845) that was computer-controlled through a digital-to-analog converter (IOtech Inc. DAC488/2). The current generated by illuminating the Chlide film adsorbed on the thiol SAM under potentiostatic conditions was amplified (current amplifier, Keithley 428), recorded (16-bit analog-to-digital converter, IOtech Inc. ADC488/8SA), visualized (oscilloscope, Tektronix TDS 340A), and stored (Power PC G3, Macintosh). Operation of the experimental setup and data acquisition were carried out under computer control (GBIP interface, National Instruments board) using a homemade acquisition program written in LabView environment. To increase the signal-to-noise ratio, current versus time curves were stored upon averaging no less than 16 current signals. The signal was usually sampled at 200-μs intervals; average standard deviations were always found to be no greater than ±2%.

The absorption spectra of Chlide were recorded using a UV−visible spectrophotometer (Cary 3, Varian). The action spectra of the stationary photocurrent of Chlide were obtained with a quartz tungsten halogen lamp (250 W, Thermo Oriel) and different narrow bandwidth interference filters from 400 to 750 nm (Lot Oriel). The monochromatic light power at the exit of the optical fiber was measured by a handheld laser power meter (Mod. Laser Check: spectral response 400−1064 nm, accuracy ±5%, power range 0.5 μW−1 W; Coherent).

Because of the high sensitivity of Chlide to the blue and red components of visible light, all measurements were carried out under green light conditions. All potentials are referred to the Ag\|AgCl\|0.1 M KCl reference electrode.

Results

Figure 1 shows a series of negative photocurrents obtained on C_{14}-coated mercury at different applied potentials over the potential range in which Chlide is electroinactive in the dark.
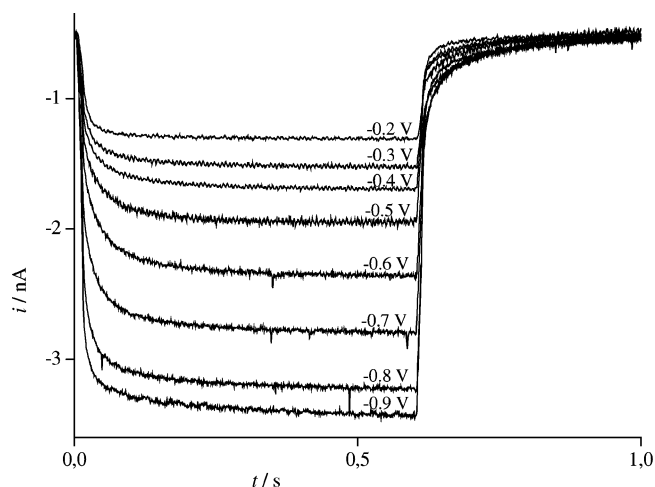
Figure 1. Light-on and light-off currents recorded upon illuminating Chlide adsorbed on C$_{14}$-coated mercury in pH 8.5 aqueous 0.1 M KCl with red light for 0.6 s at the potential reported on each curve. Measurements were carried out on the same freshly prepared drop, starting from the most positive potential and waiting for the stabilization of the background current before illuminating the drop at each potential.
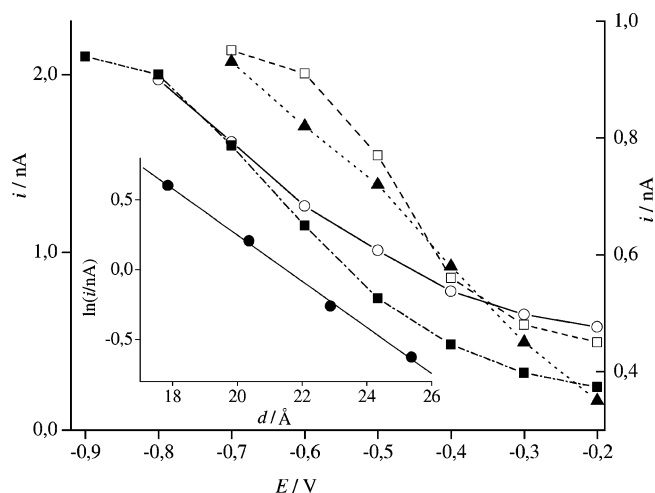

Figure 2. Plots of the stationary light-on current *i* on C$_{12}$- (○), C$_{14}$- (■), C$_{16}$- (□), and C$_{18}$-coated mercury (▲) with Chlide molecules on top, as a function of the applied potential *E*. The left-hand scale refers to C$_{12}$- and C$_{14}$-coated mercury, the right-hand one to C$_{16}$- and C$_{18}$-coated mercury. The inset shows a plot of the natural logarithm of the current *i*, measured at the potential of the Gaussian maximum, against the thickness, *d*, of the corresponding alkanethiol SAM on mercury. The thickness of a SAM with *n* carbon atoms was calculated as a sum of the following bond lengths: 0.5Hg−S (1.1 Å) + CH$_2$−S (1.5 Å) + (*n* − 1)CH$_2$−CH$_2$ (1.255 Å) + radius of the terminal methyl group (2.0 Å) (see ref 18).

The light-on current attains an almost stationary value in about 0.2 s, while the corresponding light-off current decays exponentially to zero in about the same time. The rise time of the photocurrents in Figure 1 is associated with the rise time of our instrumentation. The negative light-on current is due to the electroreduction of the photoexited Chlide molecule, Chlide*, to the corresponding radical anion, Chlide⁻, which transfers its electron to water with hydrogen evolution, thus sustaining the light-on current. Figure 2 shows plots of the stationary light-on current *i* on mercury coated with alkanethiols from C$_{12}$ to C$_{18}$, with Chlide molecules on top, as a function of the applied potential *E*. The slope of these *i* vs *E* plots tends to decrease at the most negative potentials. This behavior cannot be ascribed to depletion effects. In fact, during the flow of the stationary
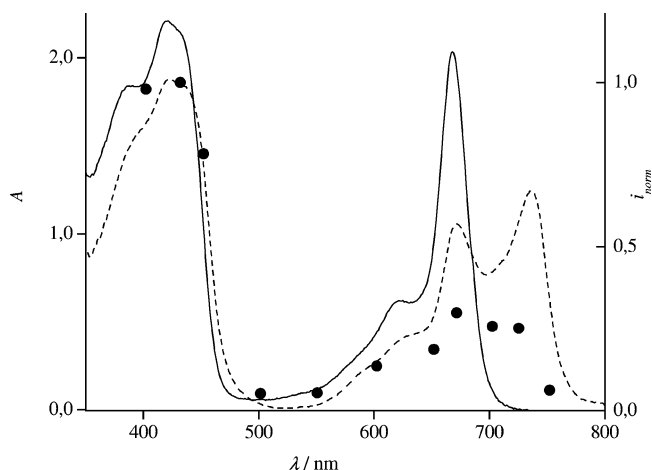

Figure 3. Action spectrum of the normalized stationary photocurrent of Chlide (●) in a pH 8.5 aqueous solution of 0.1 M KCl, and absorption spectra of 4.72 × 10⁻⁶ M (solid curve) and ∼5 × 10⁻⁵ M (dashed curve) Chlide in the same buffer solution. The action spectrum was normalized to the maximum absorbance of 5 × 10⁻⁵ M Chlide.

photocurrent, the surface concentration of adsorbed Chlide molecules is unaltered, because the electrons released from the photoexited molecules to water are continuously replaced by those provided by the electrode. For the same reason, no corrections for double-layer effects due to any change in surface concentration with varying the applied potential are required. The current *i* can, therefore, be regarded as a direct measure of the rate constant *k* for the electrode process Chlide* + e → Chlide⁻:

$$i = kA\Gamma_{\text{Chlide*}} \tag{1}$$

where $\Gamma_{\text{Chlide*}}$ is the surface concentration of Chlide* and *A* is the electrode surface area. This amounts to assuming that the rate of the reaction of the anion radical with water is so rapid that this reaction does not affect the magnitude of the steady-state photocurrents. The decrease in slope of the curves in Figure 2 is due to the fact that the driving force $-e\Delta E$, where $\Delta E \equiv E - E°$ is the difference between the applied potential *E* and the standard potential, *E*°, of the Chlide*/Chlide⁻ couple and *e* is the absolute value of the electronic charge, tends to approach, and ultimately to exceed, the reorganization energy λ for the electrode process. In other words, the overlap between the density of the electronic states in the metal and the population of photoexited Chlide molecules tends to a maximum limiting value. In contrast to homogeneous electron-transfer reactions, such an overlap cannot decrease when the driving force exceeds λ, giving rise to a Marcus inverted region, simply because tunneling from the electronic states in the metal below the Fermi level takes place even when $-e\Delta E$ exceeds λ. In other words, the inverted region of homogeneous electron-transfer reactions becomes a "saturated" region in electron-transfer reactions at electrodes.

Figure 3 shows the action spectrum of the normalized stationary photocurrent of Chlide adsorbed on top of a C$_{14}$ SAM, as obtained with a set of narrow-band interference filters. Practically identical action spectra were obtained with the other thiol SAMs. To have comparable conditions of illumination, the light power at the exit of the optical fiber was measured with each interference filter, using the same halogen lamp.

Photocurrents were then normalized to equal quantum flux density for all wavelengths adopted. For comparison, Figure 3 also shows the absorption spectra of Chlide in a pH 8.5 aqueous solution of 0.1 M KCl. The absorption spectrum of 4.72×10^{-6} M Chlide exhibits two peaks at 421 and 668 nm, whereas a saturated Chlide solution ($\sim 5 \times 10^{-5}$ M) exhibits a further peak at about 740 nm, which is ascribed to Chlide aggregates. The closer similarity of the action spectrum to the absorption spectrum of the saturated Chlide solution suggests that the Chlide molecules on top of the thiol SAM are adsorbed, at least partly, as aggregates.

An advantageous feature of monolayers self-assembled on a hanging mercury drop electrode is represented by the possibility of expanding the drop, and hence the supported film, up to a certain extent with the film still maintaining its impermeable barrier properties toward redox couples. Thus, phospholipid monolayers can be expanded up to 100%;[17] alkanethiol SAMs from C_9 to C_{14} can be expanded up to about 30%, whereas SAMs with chain length above C_{14} fracture upon drop expansion in excess of about 5%, thus behaving as essentially rigid films.[18] This abrupt passage from a liquid to a rigid state at room temperature is also revealed by the abrupt increase in the resistance of the thiol films shown in Table 1. Incidentally, the resistance of an alkanethiol monolayer is much more sensitive to the film compactness and rigidity than its differential capacity.[13] As long as the film maintains its impermeability upon drop expansion, the self-assembled molecules merely increase their tilt, while the volume of the film remains constant. This implies that the drop area A is inversely proportional to the film thickness d, and the same is true for the differential capacity C, in view of the Helmholtz formula, $C = \epsilon/(4\pi d)$. From the slope of a plot of C vs $1/d$, a dielectric constant ϵ of 2 was obtained for C_{12} and C_{14} SAMs on Hg, in agreement with the literature.[13,18,19] Figure 4 shows plots of ln i vs the thickness, d, of C_{12} and C_{14} SAMs on a progressively expanded mercury drop; the thickness was determined from differential capacity measurements using the Helmholtz formula with $\epsilon = 2$. The slopes of these plots are -0.022 Å^{-1} for C_{12} and -0.050 Å^{-1} for C_{14}.

Discussion

In general, the rate constant of a simple electron-transfer process at an electrode is expressed by the equation[11]

$$k = v \int_{-\infty}^{+\infty} \rho(\epsilon)n(\epsilon)D_{OX}(\epsilon,\lambda,\Delta E)P(\epsilon,\Delta E) \, d\epsilon \qquad (2)$$

where ϵ is the energy, v is the frequency factor, $\rho(\epsilon)$ is the density of electronic states in the metal, $n(\epsilon)$ is the probability of their being occupied, $D_{OX}(\epsilon)$ is the density of electron acceptor levels, and $P(\epsilon,\Delta E)$ is the tunneling probability. If we assume that P is practically independent of ΔE and that both P and ρ are independent of ϵ, and we express $n(\epsilon)$ by the Fermi

(17) Becucci, L.; Moncelli, M. R.; Herrero, R.; Guidelli, R. *Langmuir* **2000**, *16*, 7694–7700.
(18) Slowinski, K.; Chamberlain, R. V.; Miller, C. J.; Majda, M. *J. Am. Chem. Soc.* **1997**, *119*, 11910–11919.
(19) Porter, M. D.; Bright, T. B.; Allara, D. L.; Chidsey, C. E. D. *J. Am. Chem. Soc.* **1987**, *109*, 3559–3568.
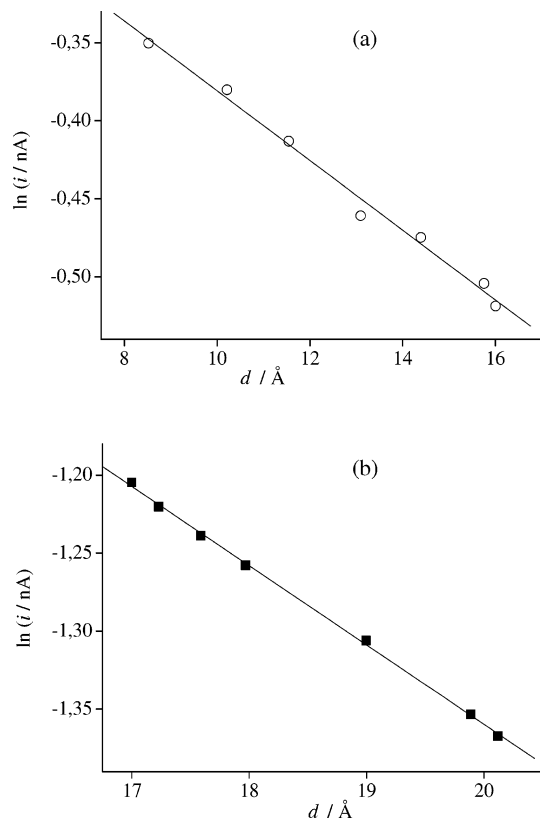
Figure 4. Plots of ln i against the thickness, d, of C_{12} (a) and C_{14} (b) SAMs on a progressively expanded mercury drop. The current i was measured at the potential of the Gaussian maximum, reported in Table 1.

distribution function and D_{OX} by Marcus's Gaussian distribution, we obtain

$$k = v\rho P \int_{-\infty}^{+\infty} \left(1 + \exp\frac{\epsilon}{k_B T}\right)^{-1}$$
$$(4\pi\lambda k_B T)^{-1/2} \exp\frac{-(\epsilon - e\Delta E - \lambda)^2}{4\lambda k_B T} \, d\epsilon \quad (3)$$

where the energy ϵ is defined relative to the Fermi level of the metal. If the Fermi distribution is approximated by a step function, then the integration is performed between $\epsilon = -\infty$ and $\epsilon = 0$, yielding

$$k(\Delta E) = \frac{v\rho P}{2} \, \text{erfc}\frac{e\Delta E + \lambda}{(4\lambda k_B T)^{1/2}} \qquad (4)$$

where $\text{erfc}(x) \equiv [1 - 2\pi^{-1/2}\int_0^x \exp(-r^2) \, dr]$ is the error function complement. For $\eta \rightarrow +\infty$, $k(\Delta E)$ tends to zero, while for $\Delta E \rightarrow -\infty$, it tends to its maximum value, $k_{max} = v\rho P$. For $\lambda = -e\Delta E$, namely when the driving force matches the reorganization energy, $k(\Delta E = -\lambda/e)$ equals one-half of its maximum value. The slope of the $k(\Delta E)$ vs ΔE plot is expressed by the equation

$$\frac{dk(\Delta E)}{d\Delta E} = -\frac{v\rho Pe}{(4\pi\lambda k_B T)^{1/2}} \exp\frac{-(e\Delta E + \lambda)^2}{4\lambda k_B T} \qquad (5)$$

According to this equation, the plot of $dk/d\Delta E$ vs ΔE is a Gaussian whose maximum lies at $\Delta E = -\lambda/e$ and whose half-width also depends on λ. Figure 5 shows plots of di/dE against
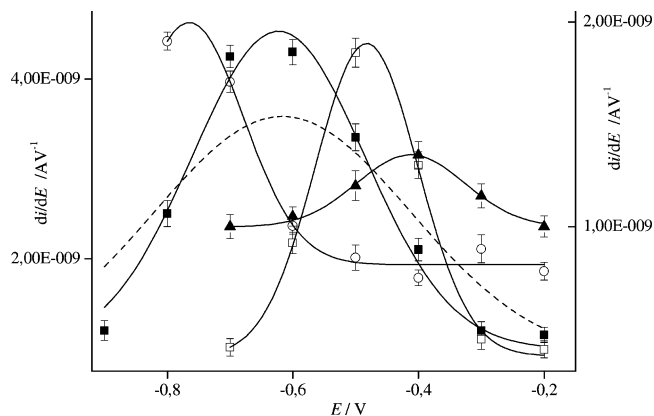
Figure 5. Plots of di/dE against E for C_{12}- (○), C_{14}- (■), C_{16}- (□), and C_{18}-coated mercury (▲), as obtained by differentiating the i vs E curves in Figure 2. The solid curves are fits of the data to the expression $\{A + B \exp[-(\lambda + e\Delta E)^2/C]\}$. The dashed curve is the best fit of the experimental di/dE vs E plot for the C_{14} SAM to the expression $\{A + B \exp[-(\lambda + e\Delta E)^2/4k_BT]\}$. The left-hand scale refers to C_{12}- and C_{14}-coated mercury, the right-hand one to C_{16}- and C_{18}-coated mercury.

E for the four different alkanethiols, as obtained by differentiating the i vs E curves in Figure 2. These plots, with the exception of that for C_{12}, show a maximum that may allow an estimate of λ from the E value corresponding to the maximum, provided the standard potential, $E°$, of the Chlide*/Chlide$^-$ couple is known. This depends on whether the photoexited Chlide* molecule is in the triplet or singlet state. The redox potentials of the Chl*/Chl$^-$ couple for the triplet and singlet states are approximately equal to $E°_3 = +0.2$ V and $E°_1 = +0.7$ V vs the Ag|AgCl|0.1M KCl electrode, and those for the Chlide*/Chlide$^-$ couple are expected to be practically the same. The di/dE vs E plots in Figure 5 were fitted to the expression $\{A + B \exp[-(\lambda + e\Delta E)^2/C]\}$, where the constant term A accounts for the background contribution to the current, and the preexponential factor B includes, among other things, the surface concentration of Chlide. The best fits, reported in the figure, were obtained by using the redox potential for the triplet state of Chl*. This result is consistent with the fact that, typically, porphyrin exited singlet states have lifetimes of a few nanoseconds[20] and decay mainly radiatively. This decay competes with intersystem crossing from singlet to triplet exited states, which undergo nonradiative decay. Hence, photoinduced stationary currents are due to electron transfer from the excited triplet state. Even with the choice of $E°_3$, the C values were found to be appreciably smaller than the $4\lambda k_BT$ values predicted by eq 5, with λ obtained from the position of the corresponding maxima. For comparison, the dashed curve in Figure 5 is the best fit of the experimental di/dE vs E plot for C_{14} to the expression $\{A + B \exp[-(\lambda + e\Delta E)^2/4\lambda k_BT]\}$; it is apparent that the slopes of the two branches of the experimental plot are appreciably steeper than those predicted by eq 5. In particular, the λ values measured from the maxima of the fitted Gaussians in Figure 5 decrease regularly by about 0.1 eV per each increment in the alkyl chain by two methylene groups (see Table 1), while the λ values measured from the width of the fitted Gaussians are appreciably smaller and do not show any particular trend with varying the length of the alkyl chain. The position of the Gaussian maximum for the C_{12} thiol is uncertain

because of the low number of experimental points; however, it certainly lies at more negative potentials than for the other thiols, thus confirming the general trend.

Deviations of the experimental Gaussians from Marcus's D_{OX} expression have been reported for several redox couples at alkanethiol-coated gold electrodes, albeit smaller and in the opposite direction.[11,21] Calculating the full integral expression in eq 3 without approximating the Fermi distribution by a step function leads to a broadening of the Gaussian peak by about 0.03 eV,[21] rather than to its narrowing. Ascribing the observed deviations to the approximation involved in the assumption of a constant density $\rho(\epsilon)$ of states in the mercury seems unrealistic, since the experimental Gaussians reported by Slowinski et al.[22] for the electroreduction of $IrCl_6^{2-}$ and $FcCH_2N(CH_3)_3^{2+}$ on C_{16}-coated mercury are in good agreement with Marcus's D_{OX} expression. The same is true for the photoinduced electroreduction of Chl molecules adsorbed on C_{12}- and C_{14}-coated mercury,[15] where the phytyl chains are quite probably intercalated with the thiol chains; here too, the experimental di/dE vs E plots (see Figure 4 of ref 15) are quite satisfactorily fitted to the expression $\{A + B \exp[-(\lambda + e\Delta E)^2/4\lambda k_BT]\}$. It should be noted that the λ values obtained from these fits exhibit an opposite trend with respect to those for Chlide electroreduction, in that λ is greater for C_{14} than for C_{12}. According to the Marcus model, the solvent contribution, λ_0, to the reorganization energy λ is given by[23,24]

$$\lambda_0 = \frac{e^2}{2}\left(\frac{1}{a} - \frac{1}{2r}\right)\left(\frac{1}{\epsilon_{op}} - \frac{1}{\epsilon_s}\right) \quad (6)$$

where a is the radius of the redox species, r is the distance to the center of the redox species from the electrode surface, and ϵ_{op} and ϵ_s are the optical and static dielectric constants of the solvent. This equation predicts an increase of λ_0 with an increase in the chain length of the alkanethiol (if $1/2r$ is not $\ll 1/a$), contrary to the behavior exhibited by the λ values for Chlide electroreduction on thiol-coated mercury.

In the proximity of the inverted region, quantum effects on the nuclear motion can be quite large.[25] Consideration of vibrational quantum effects in homogeneous electron-transfer reactions may lead to expressions for the rate constant characterized by a Gaussian exponential, $\exp[-(\Delta G° + L)^2/4MRT]$, in which L is different from M.[25-27] These expressions can be readily extended to electrode reactions by substituting $\Delta G°$ with $e\Delta E$. According to the "semiclassical treatment" proposed by Hopfield,[27] L equals λ, while M equals λ times a factor χ that is greater than unity and approaches unity for small vibrational frequencies. Hence, this treatment predicts a Gaussian curve broader than that predicted by the classical expression of eq 5 and cannot explain the present results. In the case of a highly exothermic reaction and when a single vibration frequency ν is mainly involved in the readjustment of nuclear coordinates associated with the electron transfer, an expression proposed by Marcus[26] contains a Gaussian exponential in which M is the

(20) Gust, D.; Moore, T. A.; Moore, A. L. In *Electron Transfer in Chemistry*; Balzani, V., Ed.; Wiley-VCH: Weinheim, 2001; Vol. 3, pp 272–336.

(21) Becka, A. M.; Miller, C. J. *J. Phys. Chem.* **1992**, *96*, 2657–2668.
(22) Slowinski, K.; Slowinska, K. U.; Majda, M. *J. Phys. Chem. B* **1999**, *103*, 8544–8551.
(23) Marcus, R. A. *J. Phys. Chem.* **1963**, *67*, 853–857.
(24) Marcus, R. A. *J. Chem. Phys.* **1965**, *43*, 679–701.
(25) Marcus, R. A.; Sutin, N. *Biochim. Biophys. Acta* **1985**, *811*, 265–322.
(26) Marcus, R. A. *Faraday Discuss. Chem. Soc.* **1982**, *74*, 7–15.
(27) Hopfield, J. J. *Proc. Natl. Acad. Sci. U.S.A.* **1974**, *71*, 3640–3644.

classical reorientational contribution, λ_0, of the solvent to the reorganization energy, while L equals $(\lambda_0 + v h \nu)$, where the $v h \nu$ term accounting for the effect of the high-frequency vibration can be positive. However, if we ascribe this high-frequency vibration to the inner coordination shell of Chlide, it is difficult to explain how the corresponding contribution, $v h \nu$, should decrease gradually with an increase in the thiol chain length, so as to justify the decrease in the λ value extracted from the experimental Gaussian peaks. In fact, the mode of adsorption of the Chlide molecules on top of the different alkanethiol SAMs is expected to be practically the same, as also supported by the identity of the corresponding action spectra.

A tentative explanation for the decrease in λ with an increase in the alkanethiol chain length is based on the consideration that the transition temperature from the gel to the liquid crystalline state increases with an increase in the chain length of alkanethiols, with a resulting increase in the rigidity of the corresponding SAMs. This, in turn, determines a decrease in the number of water molecules that are incorporated in the outermost portion of the SAMs. Therefore, the contribution of these molecules to the reorganization energy for the electroreduction of the Chlide* molecules adsorbed on the thiol SAM is expected to decrease. The different behavior of Chl* electroreduction on C_{12}- and C_{14}-coated Hg[15] may be ascribed to the intercalation of the phytyl chain of the adsorbed Chl molecules within the hydrocarbon chains of the thiol molecules. The different structure of the phytyl chain with respect to the chains of the n-alkanethiols is likely to create a local disorder in the SAM, which may favor the incorporation of water molecules in the proximity of the phytyl chain. It is also possible that the higher rigidity of the C_{14} SAM with respect to the C_{12} SAM may increase such a local disorder, with a resulting increase in the amount of incorporated water molecules. This may explain why the λ value for Chl* electroreduction on C_{14} (1.0 eV) is higher than that (0.76 eV) on C_{12}.

In principle, a decrease in the number of water molecules incorporated in the outermost portion of the thiol SAMs with an increase in chain length might cause a gradual change in the redox potential of the Chlide molecules adsorbed on the SAMs, which might be partially responsible for the trend in Figure 5. To verify this possibility, the experimental Gaussians were fitted to the Marcus expression, $\{A + B \exp[-(\lambda + e\Delta E)^2/4\lambda k_B T]\}$, while letting the ΔE value "float". Excellent fittings were obtained (data not shown), but neither ΔE nor λ showed a trend with an increase in chain length. Moreover, the λ values resulting from the fitting are unreasonably low ($0.12 < \lambda < 0.37$ eV), and the $E°$ values are shifted in the negative direction to an unreasonably large extent. Therefore, no attempt was made to account for the dependence of $E°$ upon chain length.

The contribution to λ from the water molecules incorporated in thiol SAMs is expected to be significant in the case of hydrophobic molecules, such as Chlide, which are "specifically" adsorbed on the SAM after depriving themselves of their hydration sheath in the direction of the SAM. In the case of hydrophilic molecules that exchange electrons with the metal in the nonadsorbed state, while retaining their hydration sheath, this contribution to λ is expected to be negligible with respect to that from the hydration sheath interposed between the redox species and the SAM. Slowinski et al.[22] observed that the λ

value for the electroreduction of the hydrophobic $FcCH_2N$-$(CH_3)_3{}^{2+}$ ion on C_{16}-coated Hg is appreciably less than that for the electroreduction of the hydrophilic $IrCl_6{}^{2-}$ ion; they explained this result on the basis of eq 6, upon considering that the radius, a, of $FcCH_2N(CH_3)_3{}^{2+}$ is greater than that of $IrCl_6{}^{2-}$. An alternative explanation may be represented by the lack of a hydration sheath interposed between the reacting species and the SAM for the ferrocene probe, but not for $IrCl_6{}^{2-}$.

In general, the tunneling probability P in eqs 3–5 decays exponentially with the distance d between the electron donor and acceptor, according to the equation

$$P = Z \exp(-\beta d) \tag{7}$$

The decay constant β is only weakly dependent on ΔE for both through-space and through-bond tunneling.[11] From eqs 4 and 7, it follows that the natural logarithm of the rate constant k at the potential of the Gaussian maximum (see Table 1) is given by

$$\ln k = \ln\left(\frac{Z v \rho}{2}\right) - \beta d \qquad \text{for } e\Delta E = -\lambda \tag{8}$$

This equation predicts that the plot of $\ln i (\Delta E = -\lambda/e)$ versus the film thickness d is linear, with slope $-\beta$. Such a plot for Chlide-photoinduced electroreduction on alkanethiol SAMs is shown in the inset of Figure 2. The slope of this linear plot yields a β value of 0.17 Å^{-1}. From the two Gaussian maxima for Chl-photoinduced electroreduction on Hg-supported C_{12} and C_{14} SAMs and from the corresponding i vs E curves in Figures 4 and 3 of ref 15, a similar β value of 0.2 Å^{-1} is obtained, although λ increases on passing from the C_{12} to the C_{14} SAM, while the opposite trend is observed with Chlide. This points out the opportunity to estimate the β value only after correcting for the reorganization energy λ, even for electron transfers relative to the same redox couple on alkanethiol monolayers of different chain lengths self-assembled on the same metal. In fact, the common procedure of plotting $\ln k$ (or $\ln i$) versus d at constant applied potential E may incorporate distance-dependent contributions, not only from P, but also from Franck–Condon factors, such as the solvent reorganization energy.

The above β values are appreciably smaller than those commonly reported for redox couples on alkanethiol-coated electrodes, which range from 0.5 to 1 Å^{-1}.[18,28–30] However, β values are often smaller when one of the reactants is electronically excited.[25] Thus, values ranging from 0.3 to 0.5 Å^{-1} have been reported in photoconduction experiments in dye-sensitized Langmuir films,[7] in fluorescence quenching experiments in which a layer of dye and a layer of acceptor were separated by a fatty acid monolayer,[8] and in photoconduction experiments in which a semitransparent aluminum electrode and an anthracene crystal were separated by a fatty acid layer.[9] This behavior can be explained by considering that luminescence can be quenched both by electron transfer and by energy transfer. So far, energy transfer from Chlide* to the metal was entirely neglected, even though its occurrence decreases the photocurrent. In particular, any dependence of the energy transfer upon

(28) Liang, C.; Newton, M. D. *J. Phys. Chem.* **1993**, *97*, 3199–3211.
(29) Salomon, A.; Cahen, D.; Lindsay, S.; Tomfohr, J.; Engelkes, V. B.; Frisbie, C. D. *Adv. Mater.* **2003**, *15*, 1881–1890.
(30) Smalley, J. F.; Finklea, H. O.; Chidsey, C. E. D.; Linford, M. R.; Creager, S. E.; Ferraris, J. P.; Chalfant, K.; Zawodzinsk, T.; Feldberg, S. W.; Newton, M. D. *J. Am. Chem. Soc.* **2003**, *125*, 2004–2013.

distance or potential will affect the distance or potential dependence of the photocurrent. There is ample evidence in the literature that the effect of a metal as an acceptor of the radiation field from a sensitizer is to decrease the lifetime of the sensitizer, more so the shorter the distance from the metal.[31−37] This increase in quenching by energy transfer with a decrease in the distance, d, is expected to induce a concomitant photocurrent decrease that partially compensates for the photocurrent increase due to the increase in the electron-transfer rate. This may explain the small β values observed in the present photoconduction experiments. On the other hand, to the authors' knowledge, no clear evidence exists for a potential dependence of the quenching by energy transfer. An expression for the luminescence lifetime near a metal surface derived by Persson and Lang[33] has the form $\tau(d) = \tau_\infty(1 + a/d^3 + b/d^4)^{-1}$, where the d^{-3} dependence accounts for the transfer of the vibrating dipole representing the sensitizer to the bulk metal, while the d^{-4} dependence, typical of the Förster-type energy transfer, accounts for the dipole transfer to the metal surface. The a coefficient in this expression depends on the permittivity of the metal at the dipole radiation frequency, while the b coefficient depends on the Fermi frequency and the Fermi wave vector of the metal, which are functions of its free electron radius. All these quantities depend on the nature of the metal,[34] but not on the applied potential.

The β values, 0.022 and 0.050 Å^{-1}, obtained from the slopes of the ln i vs d plots on C$_{12}$ and C$_{14}$ SAMs by varying d via a progressive expansion of the mercury drop (see Figure 4) are much less than that, 0.17 Å^{-1}, obtained by increasing the film thickness via an increase in the number of carbons in the alkanethiol chain (see the inset of Figure 2). This indicates unequivocally that through-bond tunneling is much more efficient than through-space tunneling. Analogous conclusions were drawn by Slowinski et al. by measuring the tunneling current for Ru(NH$_3$)$_6^{3+}$ electroreduction across a Hg-supported C$_{12}$ SAM during mercury drop expansion.[18] As concerns the decay constant, β_{TS}, for through-space (TS) tunneling with respect to that, β_{TB}, for through-bond (TB) tunneling, different conclusions may be drawn depending on the model adopted. Slowinski et al.[18] postulate a model of electron transfer in which the current follows the backbone of the thiol molecule (TB pathway), with a small "chain-to-chain" contribution (TS pathway) in the direction normal to the axis of the tilted molecules. With this model, they estimate that the β value for the more efficient TB tunneling equals $\beta_{TB} = 0.91$ Å^{-1}, while that for the less efficient TS tunneling equals $\beta_{TS} = 1.31$ Å^{-1}. On the other hand, if one assumes that TB and TS tunneling proceed independent of each other and that TS tunneling takes place along the shortest distance between the redox center and the electrode surface, then the TB tunneling does not contribute to the slope of the ln i vs d plots in the drop-expansion experiments of Figure 4. Therefore, this slope yield directly β_{TS}, which turns out to be less than β_{TB}.

In conclusion, the derivative of the stationary photocurrents due to the electroreduction of Chlide adsorbed on Hg-supported alkanethiol SAMs with respect to the applied potential, once plotted against potential, yields Gaussian curves whose maximum allows an estimate of the reorganization energy λ; this is found to decrease regularly with an increase in the thiol chain length. A tentative explanation based on a decrease in the amount of water molecules incorporated in the thiol SAM with an increase in its chain length is provided. Increasing the thickness of the alkanethiol SAM by increasing its chain length causes the photocurrent, corrected for the reorganization energy, to decay exponentially with a low decay constant β of about 0.17 Å^{-1}. This low β value can be explained by concomitant energy transfer. If the thickness of an alkanethiol monolayer is decreased by expanding the drop surface, the photocurrent increases much less than observed by decreasing the alkanethiol chain length on a nonexpanded drop, thus confirming that electron transfer takes place primarily via through-bond tunneling.

(31) Khun, H. *J. Chem. Phys.* **1970**, *53*, 101−108.
(32) Tanimura, K.; Kawai, T.; Sakata, T. *J. Phys. Chem.* **1980**, *84*, 751−756.
(33) Persson, B. N. J.; Lang, N. D. *Phys. Rev. B* **1982**, *26*, 5409−5415.
(34) Kuhnke, K.; Becker, R.; Epple, M.; Kern, K. *Phys. Rev. Lett.* **1997**, *79*, 3246−3249.
(35) Andrew, P.; Barnes, W. L. *Science* **2000**, *290*, 785−788.
(36) Imahori, H.; Norieda, H.; Nishimura, Y.; Yamazaki, I.; Higuchi, K.; Kato, N.; Motohiro, T.; Yamada, H.; Tamaki, K.; Arimura, M.; Sakata, Y. *J. Phys. Chem. B* **2000**, *104*, 1253−1260.
(37) Dulkeith, E.; Morteani, A. C.; Niedereichholz, T.; Klar, T. A.; Feldmann, J.; Levi, S. A.; van Veggel, F. C. J. M.; Reinhoudt, D. N.; Möller, M.; Gittins, D. I. *Phys. Rev. Lett.* **2002**, *89*, 203002-1−203002-4.